

# Adaptive Threshold Selection for Set Membership State Estimation with Quantized Measurements

Marco Casini, Andrea Garulli, Antonio Vicino \*

## Abstract

State estimation for discrete-time linear systems with uniformly quantized measurements is addressed. By exploiting the set-theoretic nature of the information provided by the quantizer, the problem is cast in the set membership estimation setting. Assuming the possibility of suitably tuning the quantizer range and resolution, the optimal design of adaptive quantizers is formulated in terms of the minimization of the radius of information associated to the state estimation problem. The optimal solution is derived for first-order systems and the result is exploited to design adaptive quantizers for generic systems, minimizing the size of the feasible output signal set. Then, the number of sensor thresholds for which the adaptive quantizers guarantee asymptotic boundedness of the state estimation uncertainty is established. Threshold adaptation mechanisms based on several types of outer approximations of the feasible state set are also proposed. The effectiveness of the designed adaptive quantizers is demonstrated on numerical tests, highlighting the trade off between the resulting estimation uncertainty and the computational burden required by recursive set approximations.

## 1 Introduction

The effect of quantization in control systems has been investigated since long time (see, e.g., [1,2] and references therein). In particular, it is well known that adaptive quantizers can be employed to improve the performance of the control loop [3–6]. Due to the steadily increasing diffusion of networked systems with limited communication rate, the role of quantization has been intensively studied also in system identification [7–12] and state estimation [13–16].

In estimation problems, online adaptation of the quantizer thresholds can be exploited to reduce estimation errors and improve the system performance. The problem considered in this paper is relevant to two possible application settings. The first one is that of a sensor with a limited number of quantization levels, whose thresholds can be suitably triggered. Examples of such sensors are described in [7, Chapter 1] and the threshold adaptation problem is treated in [7, Chapter 14] in the context of system identification. Another application domain is that of networked systems, such as wireless sensor networks or industrial control networks, in which quantization for communication allows the user to choose how to partition the signal range in subsets, which is equivalent to suitably select the quantizer thresholds. This has motivated a growing interest in the design of adaptive quantizers for system identification [17–21], distributed sensing [22, 23] and data converters [24]. In particular, an expectation-maximization algorithm and a quasi-Newton search are employed in [20] to obtain a parameter estimate, on the basis of which the quantizer thresholds are adapted. In [21], a similar solution is proposed, based on a stochastic gradient algorithm. Time-varying thresholds are obtained in [22] by adding a control input before sensor quantization. Three different threshold adaptation schemes for distributed parameter estimation are proposed in [23]. In the above settings, it is implicitly assumed that the

---

\*The authors are with the Dipartimento di Ingegneria dell’Informazione e Scienze Matematiche, Università di Siena, Siena, Italy. e-mail: {casini,garulli,vicino}@diism.unisi.it.

same estimation algorithm is run at both ends of the communication channel, so that the sensor can autonomously adapt the thresholds in the same way as it is done by the estimator.

In this paper, the problem of designing adaptive quantizers will be addressed in the context of set membership state estimation for discrete-time linear systems. The aim is to find an adaptation scheme for the sensor thresholds which minimizes the set-theoretic uncertainty associated to the state estimates.

## 1.1 Related work

Set membership state estimation has a long history, whose origin dates back to more than 50 years ago [25, 26]. The main idea is as follows: when the system is affected by unknown-but-bounded (UBB) process disturbance and measurement noise, it is possible to define the so-called *feasible state set*, i.e., the set of all the states that are compatible with the available input-output measurements and the disturbance bounds. An advantage of this approach is that all the elements of the feasible set can be equivalently considered as pointwise estimates of the state, depending on the specific application at hand. Different measures of the size of the feasible set can be used to quantify the uncertainty affecting the estimate. On the other hand, a major problem in set membership estimation is that feasible sets rapidly become too complex to be computed exactly. Even in the case of linear dynamic systems, feasible sets are usually polytopes with an increasing number of facets and vertices. This has generated a rich literature in which researchers have proposed a number of techniques for approximating the feasible sets. The common idea underlying these approaches is to choose a family of sets of limited complexity and compute a set within the family that contains the true feasible set. Popular approximating sets include ellipsoids [27–29], parallelotopes [30], zonotopes [31–34] and constrained zonotopes [35–37]. The interested reader is referred to [38] for a detailed survey on the subject.

The effect of measurement quantization in state estimation has been mostly addressed in the stochastic framework. Since the seminal work in [13], the objective has been to design the quantizer parameters so that the estimation error possesses some desirable properties (typically, a bounded covariance). By leveraging the set-theoretic nature of the information provided by quantized sensor measurements, a natural alternative is to cast the state estimation problem in a deterministic setting. Recently, this approach has been proposed for state estimation based on binary sensor measurements, in the presence of UBB disturbances, leading to deterministic bounds on the estimation errors [39, 40]. A further step is to formulate the state estimation problem in the set membership estimation framework, which allows to characterize the uncertainty associated to the state estimates in terms of feasible state sets. Quite interestingly, the possibility of adopting a set membership approach when dealing with quantized measurements was already mentioned in [14], which however considered a very specific system class (cascaded integrators). A set-valued observer for linear systems with quantized measurements was first proposed in [41]. In [42] a set membership state estimation algorithm is presented, assuming that quantized measurements of all the state variables are available and that such measurements always remain in the quantizer range. In all these works, the quantizer thresholds are fixed a priori. In [43], a strategy for adapting the threshold of a binary sensor to minimize the size of the feasible state set is proposed.

## 1.2 Paper contribution

In this paper, the state estimation problem with uniformly quantized measurements is addressed for linear discrete-time systems affected by UBB disturbances. The problem is cast in the set membership estimation framework. Assuming that the thresholds of the quantizer can be adapted online, the optimal design of the quantizer parameters (range and resolution) is formulated in terms of the minimization of the *radius of information*, i.e., the radius of the feasible state set corresponding to the worst-case realization of the quantized measurements. To the best of our knowledge, the design of adaptive quantizers has never been studied in a set-theoretic framework. First, a complete solution is provided for first-order systems. Then, such a result is exploited to design adaptive quantizers for general  $n$ -th order systems, by minimizing the radius of the

feasible output signal set, namely, the set of feasible values of the (unaccessible) output signal. Moreover, it is shown that such a design guarantees asymptotic boundedness of the feasible state set, and hence of the uncertainty affecting the state estimate, provided that the quantizer has a sufficient number of thresholds. The threshold adaptation mechanism is also applied to outer approximations of the feasible state sets, computed by recursive approximation algorithms based on parallelotopes, zonotopes and constrained zonotopes. In particular, analytical expressions of the time-varying thresholds are derived for parallelotopes and zonotopes, thus making the computational burden of online adaptation negligible. The effectiveness of the proposed techniques for designing and adapting the quantizer parameters is demonstrated via numerical simulations on a specific case study and on randomly generated systems with multiple process disturbances and quantized measurements. The results provide empirical evidence that the proposed approach outperforms the results obtained by set membership estimators based on fixed thresholds.

Summing up, the contributions of the paper are:

- i) the formulation and solution of the optimal design of adaptive quantizers, for set membership state estimation of linear systems with quantized measurements (Theorems 1 and 3);
- ii) results showing that the proposed optimal adaptive quantizers guarantee asymptotic boundedness of the feasible state set, even in the case of unstable systems (Theorems 2 and 4);
- iii) an effective and computationally viable way to select the quantizer thresholds, based on commonly employed outer approximations of the feasible state set.

The rest of the paper is organized as follows. Section 2 introduces some preliminary material on set manipulations. The optimal threshold selection problem is formulated in Section 3. The problem solution is derived in Section 4 for first-order systems, and then extended to linear systems of arbitrary dimension in Section 5. The threshold selection mechanism based on outer approximations of the feasible state set is illustrated in Section 6. Numerical simulations are presented in Section 7, while Section 8 contains some concluding remarks and suggests possible future developments.

## 2 Definitions and preliminaries

The notation adopted in the paper is standard. For  $x \in \mathbb{R}$ ,  $\lfloor x \rfloor$  is the largest integer less than or equal to  $x$ . A closed interval in  $\mathbb{R}$  is denoted as  $[a, b] = \{x \in \mathbb{R} : a \leq x \leq b\}$ . Given a vector  $v \in \mathbb{R}^n$ ,  $\text{diag}(v)$  is a diagonal matrix with diagonal equal to  $v$ . The transpose of  $v$  is denoted by  $v'$ . The  $p$ -norm of  $v$  is  $\|v\|_p$  (the subscript is omitted when  $p = 2$ ). The column vector of ones is denoted by  $\mathbf{1} = [1 \ 1 \ \dots \ 1]'$ . The unit ball in the infinity norm is  $\mathcal{B}_\infty = \{x : \|x\|_\infty \leq 1\}$ .

Given sets  $\mathcal{V}, \mathcal{W} \subseteq \mathbb{R}^n$ , we define their Minkowski sum as

$$\mathcal{V} \oplus \mathcal{W} = \{z \in \mathbb{R}^n : z = v + w, \forall v \in \mathcal{V}, \forall w \in \mathcal{W}\}, \quad (1)$$

and the linear set transformation with matrix  $A \in \mathbb{R}^{m \times n}$  as

$$A\mathcal{V} = \{z \in \mathbb{R}^m : z = Av, \forall v \in \mathcal{V}\}. \quad (2)$$

The *radius* of a set  $\mathcal{V}$  is defined as

$$\text{rad}(\mathcal{V}) = \inf_z \sup_{v \in \mathcal{V}} \|z - v\|. \quad (3)$$

The argument  $z$  of the infimum in (3) is the *center* of  $\mathcal{V}$ .

Given  $p \in \mathbb{R}^n$  and  $\gamma \in \mathbb{R}$ , a *strip* is defined as

$$\mathcal{S}(p, \gamma) = \{x \in \mathbb{R}^n : |p'x - \gamma| \leq 1\}. \quad (4)$$

A non-degenerate *parallelotope* is the intersection of  $n$  linearly independent strips. Given  $c \in \mathbb{R}^n$  and a nonsingular matrix  $P \in \mathbb{R}^{n \times n}$ , it is defined as

$$\begin{aligned} \mathcal{P}(P, c) &= \{x \in \mathbb{R}^n : \|Px - c\|_\infty \leq 1\} \\ &= \{x \in \mathbb{R}^n : x = x_c + T\alpha, \|\alpha\|_\infty \leq 1\} \end{aligned} \quad (5)$$

where  $T = P^{-1}$  and  $x_c = P^{-1}c$ . Its radius is given by

$$\text{rad}(\mathcal{P}(P, c)) = \max_{w \in \mathcal{B}_\infty} \|P^{-1}w\|. \quad (6)$$

Moreover, for any vector  $v \in \mathbb{R}^n$ , it holds

$$\sup_{x \in \mathcal{P}} v'x - \inf_{x \in \mathcal{P}} v'x = 2\|v'P^{-1}\|_1. \quad (7)$$

A *zonotope* [31] is an extension of a parallelotope, defined as

$$\mathcal{Z}(T, x_c) = \{x \in \mathbb{R}^n : x = x_c + T\alpha, \|\alpha\|_\infty \leq 1\} \quad (8)$$

where  $T \in \mathbb{R}^{n \times m}$  and  $\alpha \in \mathbb{R}^m$ . The columns of  $T$  are the generators of the zonotope and its order is  $o = \frac{m}{n}$ .

A *constrained zonotope* [35] is an extension of a zonotope, defined as

$$\mathcal{CZ}(T, x_c, A, b) = \{x \in \mathbb{R}^n : \begin{aligned} x &= x_c + T\alpha, \\ \|\alpha\|_\infty &\leq 1, \quad A\alpha = b \end{aligned}\} \quad (9)$$

where  $A \in \mathbb{R}^{n_c \times m}$  and  $b \in \mathbb{R}^{n_c}$ . The order of a constrained zonotope is defined as  $o = \frac{m - n_c}{n}$ , where  $n_c$  is the number of equality constraints in (9).

**Proposition 1** *Given a strip  $\mathcal{S}(p, c) \subset \mathbb{R}^n$ , a nonsingular matrix  $A \in \mathbb{R}^{n \times n}$ , a matrix  $G \in \mathbb{R}^{n \times m}$  and a constant  $\gamma > 0$ , one has*

$$\begin{aligned} A\mathcal{S}(p, c) \oplus \gamma G\mathcal{B}_\infty &= \\ \{x \in \mathbb{R}^n : |p'A^{-1}x - c| \leq 1 + \gamma\|p'A^{-1}G\|_1\}. \end{aligned} \quad (10)$$

*Proof:* See Appendix .1. □

### 3 Problem formulation

Consider the discrete-time linear system

$$x(k+1) = Ax(k) + Gw(k) \quad (11)$$

$$z(k) = Cx(k) + v(k) \quad (12)$$

where  $x(k) \in \mathbb{R}^n$  is the state vector,  $z(k) \in \mathbb{R}$  is the (inaccessible) output signal,  $w(k) \in \mathbb{R}^m$  is the process disturbance and  $v(k) \in \mathbb{R}$  is the output noise. In the case of multi-output systems, the results presented in the paper can be applied by processing sequentially the output measurements, at the price of a higher conservativeness of the uncertainty estimates (see Section 7.2).

The process disturbance  $w(k)$  and the output noise  $v(k)$  are unknown-but-bounded (UBB) sequences, i.e. they satisfy

$$\|w(k)\|_\infty \leq \delta_w \quad (13)$$

$$|v(k)| \leq \delta_v \quad (14)$$

for all  $k \geq 0$ .

Observations of the output signal are obtained from a quantized sensor with  $d$  thresholds  $\tau_1, \dots, \tau_d$ , such that

$$y(k) = \sigma(z(k)) \triangleq \begin{cases} 0 & \text{if } z(k) \leq \tau_1 \\ 1 & \text{if } \tau_1 < z(k) \leq \tau_2 \\ \vdots & \\ d & \text{if } z(k) > \tau_d. \end{cases} \quad (15)$$

The quantization is assumed to be uniform in the range  $[\tau_1, \tau_d]$ , i.e., the sensor thresholds satisfy  $\tau_{i+1} - \tau_i = \Delta$ , for  $i = 1, \dots, d-1$  and  $\Delta > 0$ . Therefore, the quantizer is defined by choosing the center of the quantizer range  $\tau_c = \frac{\tau_1 + \tau_d}{2}$  and the resolution  $\Delta$ , thus meaning that it is fully characterized by the parameter vector  $\theta = \begin{bmatrix} \tau_c \\ \Delta \end{bmatrix}$ . Then, the thresholds can be expressed in terms of  $\theta$  as

$$\tau_i = \tau_c - \left( \frac{d+1}{2} - i \right) \Delta, \quad i = 1, \dots, d. \quad (16)$$

According to the set membership estimation paradigm, the information provided by the quantized measurement  $y(k)$  is captured by the *feasible measurement set*, i.e., the set of states  $x(k)$  which are compatible with  $y(k)$ . By using (12) and (14), this is given by

$$\mathcal{M}(k) = \left\{ x \in \mathbb{R}^n : \begin{cases} Cx \leq \tau_1 + \delta_v & \text{if } y(k) = 0 \\ \tau_1 - \delta_v \leq Cx \leq \tau_2 + \delta_v & \text{if } y(k) = 1 \\ \vdots & \\ Cx \geq \tau_d - \delta_v & \text{if } y(k) = d \end{cases} \right\} \quad (17)$$

in which all strict inequalities have been transformed into nonstrict ones, in order to deal only with closed feasible sets. The set  $\mathcal{M}(k)$  is a strip in the state space when  $1 \leq y(k) \leq d-1$ , and a half-space when  $y(k) = 0$  or  $y(k) = d$  (notice that this occurs even in the noiseless case  $\delta_v = 0$ ). This justifies the set membership approach to the state estimation problem. In particular, it is possible to compute the *feasible state set*, i.e., the set of all the state vectors compatible with the available information. Let us denote by  $\Xi(k|k)$  and  $\Xi(k+1|k)$  the sets of states  $x(k)$  and  $x(k+1)$ , respectively, which are compatible with the quantized measurements collected up to time  $k$ . Such sets are defined by the recursion

$$\Xi(k|k) = \Xi(k|k-1) \cap \mathcal{M}(k) \quad (18)$$

$$\Xi(k+1|k) = A\Xi(k|k) \oplus \delta_w G\mathcal{B}_\infty \quad (19)$$

which is initialized by choosing a set  $\Xi(0|-1)$ , containing all the feasible initial states  $x(0)$ . Hereafter, we will denote  $\rho(k) = \text{rad}(\Xi(k|k))$ . By choosing the center of  $\Xi(k|k)$  as a pointwise estimate of the state  $x(k)$ ,  $\rho(k)$  represents the maximum uncertainty associated to the estimate.

If the parameter vector  $\theta$  of the quantizer is kept constant, the evolution of the feasible state sets in (18)-(19) may show undesired behaviors. For example, it may happen that the feasible set tends to become asymptotically unbounded, as in the following example.

**Example 1** Let  $n = 1$ ,  $A = G = C = 1$ ,  $\delta_w = 1$ ,  $\delta_v = 0$ . Assume  $x(0) = \frac{1}{2}$  and  $w(k) = 1$ ,  $\forall k \geq 0$ , so that  $z(k) = x(k) = \frac{1}{2} + k$ . Consider the quantizer in (15) with  $d = 3$ ,  $\tau_1 = -1$ ,  $\tau_2 = 0$ ,  $\tau_3 = 1$ . Then,  $y(0) = 2$  and  $y(k) = 3$ ,  $\forall k \geq 1$ . Hence  $\mathcal{M}(0) = [0, 1]$  and  $\mathcal{M}(k) = \{x : x \geq 1\}$ ,  $\forall k \geq 1$ . By choosing  $\Xi(0|-1) = [0, 1]$  and applying the recursion (18)-(19), one gets the sequence of feasible state sets  $\Xi(k|k) = [1, k+1]$ , for  $k \geq 1$ , which is asymptotically unbounded. This means that the uncertainty associated to any estimate of  $x(k)$  will diverge, irrespectively of the adopted estimation algorithm.

For the reasons exposed above, it is of interest to adapt the quantizer parameters in order to minimize the size of the feasible state set. Let us assume that at each time  $k$  it is possible to

choose the parameters of the quantizer  $\theta(k) = \begin{bmatrix} \tau_c(k) \\ \Delta(k) \end{bmatrix}$ . The aim is to select  $\theta(k)$  online in order to minimize the size of the resulting feasible set  $\Xi(k|k)$ . Since  $\mathcal{M}(k)$  depends on the actual value taken by the output  $y(k)$ , which in turn depends on the feasible predicted states  $\Xi(k|k-1)$  and the realization of the measurement noise  $v(k)$ , a meaningful objective is to minimize the radius of  $\Xi(k|k)$  with respect to the worst-case value taken by  $y(k)$ , i.e., to select

$$\theta^*(k) = \arg \inf_{\theta} \sup_{y(k)} \rho(k; \theta, y(k)) \quad (20)$$

where

$$\rho(k; \theta, y(k)) = \text{rad}(\Xi(k|k)) = \text{rad}(\Xi(k|k-1) \cap \mathcal{M}(k)),$$

in which the dependence of the radius on both  $\theta$  and  $y(k)$ , through  $\mathcal{M}(k)$  in (17), has been made explicit. Notice that in the information-based complexity framework, this corresponds to trigger the quantizer in order to minimize the so-called *radius of information* [44, 45]. In the next section, the solution of problem (20) is derived for first-order systems.

## 4 Optimal adaptive quantizer for first-order systems

Let  $n = m = 1$ . Without loss of generality, consider the system

$$x(k+1) = ax(k) + w(k) \quad (21)$$

$$z(k) = x(k) + v(k) \quad (22)$$

with  $|w(k)| \leq \delta_w$ ,  $|v(k)| \leq \delta_v$ ,  $\forall k \geq 0$ , and  $a \in \mathbb{R}$ . For ease of exposition, let us assume  $a > 0$ . If  $\Xi(0|-1) \subset \mathbb{R}$  is an interval, then all feasible sets  $\Xi(k|k)$  and  $\Xi(k+1|k)$  are also intervals. Hence, let us adopt the notation  $\Xi(k|k) = [l(k), r(k)]$ , whose radius is  $\rho(k) = (r(k) - l(k))/2$ .

The next theorem provides a solution of problem (20).

**Theorem 1** *Consider system (21)-(22) with the quantized sensor (15). Let (13)-(14) hold, with known bounds  $\delta_w, \delta_v$ . If  $a\rho(k-1) + \delta_w > \delta_v$ , a solution of problem (20) is given by*

$$\tau_c(k) = a \frac{l(k-1) + r(k-1)}{2}, \quad (23)$$

$$\Delta(k) = \frac{2}{d+1} (a\rho(k-1) + \delta_w - \delta_v). \quad (24)$$

When  $a\rho(k-1) + \delta_w \leq \delta_v$ , any  $\theta(k)$  with  $\tau_c(k)$  given by (23) and  $\Delta(k) > 0$  is an optimal solution of (20).

*Proof:* By applying (21) to  $\Xi(k-1|k-1)$ , one has

$$\begin{aligned} \Xi(k|k-1) &= [al(k-1) - \delta_w, ar(k-1) + \delta_w] = \\ &= [l(k|k-1), r(k|k-1)] \end{aligned} \quad (25)$$

whose radius is  $(r(k|k-1) - l(k|k-1))/2 = a\rho(k-1) + \delta_w$ . Problem (20) requires to select  $\theta(k)$  in order to minimize the worst-case radius of the interval  $\Xi(k|k) = \Xi(k|k-1) \cap \mathcal{M}(k)$ , for all possible values taken by the quantized output signal  $y(k)$ . By using (17) one has

$$\Xi(k|k) = \begin{cases} [l(k|k-1), \min\{\tau_1 + \delta_v, r(k|k-1)\}] & \text{if } y(k) = 0, \\ [\max\{l(k|k-1), \tau_i - \delta_v\}, \\ \min\{\tau_{i+1} + \delta_v, r(k|k-1)\}] & \text{if } y(k) = i, 1 \leq i \leq d-1, \\ \vdots \\ [\max\{l(k|k-1), \tau_d - \delta_v\}, r(k|k-1)] & \text{if } y(k) = d. \end{cases} \quad (26)$$

By adopting a simple geometric argument, the thresholds of the quantizer should be symmetrically distributed over  $\Xi(k|k-1)$  in order to provide a solution to problem (20). Therefore, the center  $\tau_c$  of the quantizer range must coincide with the center of  $\Xi(k|k-1)$  in (25), from which (23) follows.

In order to prove (24), let us compute  $\rho(k) = \text{rad}(\Xi(k|k))$  for the different outcomes of the quantized sensor  $y(k)$ . When  $y(k) = 0$ , by using (16) with  $i = 1$  and (23), from (26) one gets

$$\begin{aligned}\rho(k) &= \frac{1}{2} \min\{r(k|k-1) - l(k|k-1), \tau_1 + \delta_v - l(k|k-1)\} \\ &= \frac{1}{2} \min\{2a\rho(k-1) + 2\delta_w, \\ &\quad \tau_c(k) - \left(\frac{d-1}{2}\right) \Delta + \delta_v - al(k-1) + \delta_w\} \\ &= \min\{a\rho(k-1) + \delta_w, \\ &\quad \frac{1}{2} [a\rho(k-1) + \delta_w + \delta_v - \frac{d-1}{2} \Delta(k)]\}.\end{aligned}$$

For  $y(k) = d$  the derivation is analogous and leads to the same result. For  $y(k) = i$ , with  $1 \leq i \leq d-1$ , one gets

$$\begin{aligned}\rho(k) &= \frac{1}{2} \min\{r(k|k-1) - l(k|k-1), \tau_{i+1} - \tau_i + 2\delta_v, \\ &\quad \tau_{i+1} + \delta_v - l(k|k-1), r(k|k-1) - \tau_i + \delta_v\} \\ &= \frac{1}{2} \min\{2a\rho(k-1) + 2\delta_w, \Delta + 2\delta_v, \\ &\quad \tau_c(k) - \left(\frac{d-1}{2} - y(k)\right) \Delta + \delta_v - al(k-1) + \delta_w, \\ &\quad ar(k-1) + \delta_w - \tau_c(k) + \left(\frac{d+1}{2} - y(k)\right) \Delta + \delta_v\} \\ &= \min\{a\rho(k-1) + \delta_w, \frac{1}{2} \Delta(k) + \delta_v, \\ &\quad \frac{1}{2} [a\rho(k-1) + \delta_w + \delta_v + \frac{1}{2} \Delta(k) - |\frac{d}{2} - y(k)| \Delta(k)]\}.\end{aligned}$$

Summing up, the radius of  $\Xi(k|k)$  is equal to

$$\rho(k) = \begin{cases} \min\{a\rho(k-1) + \delta_w, \\ \quad \frac{1}{2} (a\rho(k-1) + \delta_w + \delta_v - \frac{d-1}{2} \Delta(k))\} \\ \quad \text{if } y(k) \in \{0, d\}, \\ \min\{\frac{1}{2} \Delta(k) + \delta_v, a\rho(k-1) + \delta_w, \\ \quad \frac{1}{2} [a\rho(k-1) + \delta_w + \delta_v - (|\frac{d}{2} - y(k)| - \frac{1}{2}) \Delta(k)]\} \\ \quad \text{if } y(k) \in \{1, \dots, d-1\}. \end{cases} \quad (27)$$

Let us now distinguish two cases. If  $a\rho(k-1) + \delta_w \leq \delta_v$ , for  $y(k) = \lfloor \frac{d}{2} \rfloor$  one has that (27) yields

$$\rho(k) = \begin{cases} \min\{\frac{1}{2} \Delta(k) + \delta_v, a\rho(k-1) + \delta_w, \\ \quad \frac{1}{2} [a\rho(k-1) + \delta_w + \delta_v + \frac{1}{2} \Delta(k)]\} \text{ if } d \text{ is even,} \\ \min\{\frac{1}{2} \Delta(k) + \delta_v, a\rho(k-1) + \delta_w, \\ \quad \frac{1}{2} [a\rho(k-1) + \delta_w + \delta_v]\} \text{ if } d \text{ is odd.} \end{cases}$$

Hence, using condition  $a\rho(k-1) + \delta_w \leq \delta_v$  one has  $\rho(k) = a\rho(k-1) + \delta_w$ . For all other outcomes of  $y(k) \neq \lfloor \frac{d}{2} \rfloor$ , all the expressions of  $\rho(k)$  in (27) involve the minimum between  $a\rho(k-1) + \delta_w$  and other quantities. Therefore,

$$\sup_{y(k)} \rho(k) = a\rho(k-1) + \delta_w. \quad (28)$$

Since the expression in (28) does not depend on  $\Delta(k)$ , any value of  $\Delta(k)$  is optimal.

Conversely, let us consider the case  $a\rho(k-1) + \delta_w > \delta_v$ . From (27) one gets

$$\rho(k) = \begin{cases} \frac{1}{2} (a\rho(k-1) + \delta_w + \delta_v - \frac{d-1}{2} \Delta(k)) \\ \quad \text{if } y(k) \in \{0, d\}, \\ \min\{\frac{1}{2} \Delta(k) + \delta_v, a\rho(k-1) + \delta_w, \\ \quad \frac{1}{2} [a\rho(k-1) + \delta_w + \delta_v - (|\frac{d}{2} - y(k)| - \frac{1}{2}) \Delta(k)]\} \\ \quad \text{if } y(k) \in \{1, \dots, d-1\}. \end{cases} \quad (29)$$

Let us assume that  $d$  is odd. Then, the term  $(|\frac{d}{2} - y(k)| - \frac{1}{2})$  is equal to zero when either  $y(k) = \lfloor \frac{d}{2} \rfloor$  or  $y(k) = \lfloor \frac{d+1}{2} \rfloor$ , while it is positive for any other value taken by  $y(k)$ . Therefore, from the lower term in (29), one has

$$\begin{aligned} \sup_{y(k) \in \{1, \dots, d-1\}} \rho(k) &= \\ &= \min \left\{ \frac{1}{2} \Delta(k) + \delta_v, a\rho(k-1) + \delta_w, \right. \\ &\quad \left. \frac{1}{2} [a\rho(k-1) + \delta_w + \delta_v] \right\} \\ &= \min \left\{ \frac{1}{2} \Delta(k) + \delta_v, \frac{1}{2} [a\rho(k-1) + \delta_w + \delta_v] \right\} \end{aligned}$$

where the last equality stems from the assumption  $a\rho(k-1) + \delta_w > \delta_v$ . By comparing the two terms in the right hand side one gets

$$\begin{aligned} \sup_{y(k) \in \{1, \dots, d-1\}} \rho(k) &= \\ &= \begin{cases} \frac{1}{2} \Delta(k) + \delta_v & \text{if } \Delta(k) \leq a\rho(k-1) + \delta_w - \delta_v, \\ \frac{1}{2} (a\rho(k-1) + \delta_w + \delta_v) & \text{if } \Delta(k) \geq a\rho(k-1) + \delta_w - \delta_v. \end{cases} \end{aligned} \quad (30)$$

Now, observe that the upper term in (29) is a decreasing function of  $\Delta(k)$ , while the upper term in (30) is an increasing function of  $\Delta(k)$  and the lower term in (30) does not depend on  $\Delta(k)$ . By direct comparison of such terms, one obtains

$$\sup_{y(k)} \rho(k) = \begin{cases} \frac{1}{2} (a\rho(k-1) + \delta_w + \delta_v - \frac{d-1}{2} \Delta(k)) & \text{if } \Delta(k) \leq \frac{2}{d+1} (a\rho(k-1) + \delta_w - \delta_v), \\ \frac{1}{2} \Delta(k) + \delta_v & \text{if } \frac{2}{d+1} (a\rho(k-1) + \delta_w - \delta_v) \leq \Delta(k) \leq \\ \leq a\rho(k-1) + \delta_w - \delta_v, \\ \frac{1}{2} (a\rho(k-1) + \delta_w + \delta_v) & \text{if } \Delta(k) \geq a\rho(k-1) + \delta_w - \delta_v. \end{cases} \quad (31)$$

By applying the same procedure when  $d$  is even, one gets

$$\sup_{y(k)} \rho(k) = \begin{cases} \frac{1}{2} (a\rho(k-1) + \delta_w + \delta_v - \frac{d-1}{2} \Delta(k)) & \text{if } \Delta(k) \leq \frac{2}{d+1} (a\rho(k-1) + \delta_w - \delta_v), \\ \frac{1}{2} \Delta(k) + \delta_v & \text{if } \frac{2}{d+1} (a\rho(k-1) + \delta_w - \delta_v) \leq \Delta(k) \leq \\ \leq 2(a\rho(k-1) + \delta_w - \delta_v), \\ a\rho(k-1) + \delta_w & \text{if } \Delta(k) \geq 2(a\rho(k-1) + \delta_w - \delta_v). \end{cases} \quad (32)$$

Finally, one can observe that both (31) and (32) are piecewise linear functions of  $\Delta(k)$ , whose minimum is attained for  $\Delta(k) = \frac{2}{d+1} (a\rho(k-1) + \delta_w - \delta_v)$ , which corresponds to (24).  $\square$

The rationale behind the quantizer adaptation (23)-(24) is clarified by the following example.

**Example 2** Let  $a = 2$ ,  $\delta_w = 1$ ,  $\delta_v = 2$ . Assume that at time  $k-1$  one has  $\Xi(k-1|k-1) = [-5, 5]$ . Then, from (25) one gets  $\Xi(k|k-1) = [-11, 11]$ . By applying (23)-(24) with  $d = 5$ , one has  $\tau_c(k) = 0$  and  $\Delta(k) = 3$ . The resulting thresholds  $\tau_i(k)$  in (16) are equal to  $-6, -3, 0, 3, 6$ . It is worth stressing that such thresholds do not partition the predicted feasible set  $\Xi(k|k-1)$  in equal parts. Rather, they are selected in such a way that the corrected feasible set  $\Xi(k|k) = \Xi(k|k-1) \cap \mathcal{M}(k)$  has always the same radius, equal to  $\frac{1}{2} \Delta(k) + \delta_v = \frac{7}{2}$ , irrespectively of the sensor output  $y(k)$ , thus achieving the optimal solution of problem (20).

By using the result in Theorem 1 it is possible to establish conditions for the asymptotic boundedness of the feasible set  $\Xi(k|k)$ .

**Theorem 2** *By choosing the quantizer parameters as in (23)-(24), the radius of information  $\bar{\rho}(k) = \sup_{y(k)} \rho(k)$  evolves according to*

$$\bar{\rho}(k) = \begin{cases} a\bar{\rho}(k-1) + \delta_w & \text{if } \bar{\rho}(k-1) \leq \frac{\delta_w - \delta_v}{a}, \\ \frac{1}{d+1} (a\bar{\rho}(k-1) + \delta_w + d\delta_v) & \text{if } \bar{\rho}(k-1) \geq \frac{\delta_w - \delta_v}{a}. \end{cases} \quad (33)$$

Moreover, if  $d > a - 1$ , one has

$$\lim_{k \rightarrow +\infty} \bar{\rho}(k) = \begin{cases} \frac{1}{1-a} \delta_w & \text{if } \delta_w \leq (1-a)\delta_v, \\ \frac{1}{d+1-a} (\delta_w + d\delta_v) & \text{if } \delta_w > (1-a)\delta_v, \end{cases} \quad (34)$$

and if  $\delta_w > (1-a)\delta_v$ ,

$$\lim_{k \rightarrow +\infty} \sup_{y(k)} \Delta(k) = \frac{2}{d+1-a} (\delta_w + (a-1)\delta_v). \quad (35)$$

*Proof:* Expression (33) is obtained from (28) and (31)-(32), by substituting the optimal value of  $\Delta(k)$  in (24) into (31)-(32). Then, (34) follows from standard arguments on the asymptotic behavior of system (33). Finally, (35) is obtained by substituting the second expression in (34) into (24). Note that when the first expression in (34) holds, the choice of  $\Delta(k)$  becomes asymptotically irrelevant.  $\square$

Theorem 2 states that in order to guarantee asymptotic boundedness of the feasible state set, the number of thresholds of a uniform quantizer must exceed  $a - 1$ . Notice that if system (21) is stable, this condition is always satisfied. Conversely, in the special case of a binary sensor ( $d = 1$ ), asymptotic boundedness holds if and only if  $a < 2$ .

**Remark 1** *If  $a < 0$ , the results in Theorems 1 and 2 still hold with few amendments. In particular,  $\tau_c(k)$  in (23) remains the same, while the optimal quantizer resolution becomes  $\Delta(k) = \frac{2}{d+1} (|a|\rho(k-1) + \delta_w - \delta_v)$ . Similarly, (33)-(35) hold if one replaces  $a$  with  $|a|$  in all the expressions.*

**Remark 2** *The result (34) in Theorem 2 can be seen as the set-theoretic counterpart of that in [13, Th. 3] for a stochastic estimation framework. In fact, the latter result provides the minimum number  $n$  of bits for a coder-estimator guaranteeing asymptotic boundedness of the covariance of the state estimation error. Specifically, under the assumption that all the involved stochastic disturbances have a finite-support density function, it is shown that  $2^n > a$  implies asymptotic stability of a coder estimator for a first-order system with pole  $a$ . By observing that an  $n$ -bit coder corresponds to a quantizer with  $d = 2^n - 1$  thresholds, the condition  $d > a - 1$  is recovered. In addition, Theorem 2 provides exact asymptotic expressions for the worst-case uncertainty  $\bar{\rho}(k)$  and quantizer resolution  $\Delta(k)$ , in the considered set-theoretic framework.*

## 5 General case

The solution of problem (20) in the general case of  $n$ -th order systems is intractable, because it involves a nonconvex min-max optimization over  $n$ -dimensional sets. Nevertheless, we can leverage the solution for first-order systems, in order to solve an alternative formulation of the problem, which is both meaningful and computationally feasible.

Instead of minimizing the radius of the feasible state set at time  $k$ , the aim is to minimize the radius of the *feasible output signal set*, i.e., the set of feasible values that the nominal output  $\bar{z}(k) = Cx(k)$  can take at time  $k$ . This is given by

$$\begin{aligned} C\Xi(k|k) &= C(\Xi(k|k-1) \cap \mathcal{M}(k)) \\ &= C\Xi(k|k-1) \cap C\mathcal{M}(k) \end{aligned} \quad (36)$$

where the last equality follows from the definition of  $\mathcal{M}(k)$  in (17). Then, one can design the quantizer parameters according to

$$\begin{aligned} \theta^*(k) &= \arg \inf_{\theta} \sup_{y(k)} \text{rad}(C\Xi(k|k)) \\ &= \arg \inf_{\theta} \sup_{y(k)} \text{rad}\left(C\Xi(k|k-1) \cap C\mathcal{M}(k)\right). \end{aligned} \quad (37)$$

From a geometric viewpoint, the difference between problems (20) and (37) is that the latter minimizes the projection of the uncertainty set onto the output measurement manifold. The next result provides a solution of problem (37).

**Theorem 3** Consider system (11)-(12) with the quantized sensor (15). Let

$$\bar{l}(k) = \inf_{x \in \Xi(k|k-1)} Cx, \quad \bar{r}(k) = \sup_{x \in \Xi(k|k-1)} Cx. \quad (38)$$

Then, if  $\bar{r}(k) - \bar{l}(k) > 2\delta_v$ , a solution of problem (37) is given by

$$\tau_c(k) = \frac{\bar{l}(k) + \bar{r}(k)}{2}, \quad (39)$$

$$\Delta(k) = \frac{\bar{r}(k) - \bar{l}(k) - 2\delta_v}{d+1}. \quad (40)$$

When  $\bar{r}(k) - \bar{l}(k) \leq 2\delta_v$ , any  $\theta(k)$  with  $\tau_c(k)$  given by (39) and  $\Delta(k) > 0$  is an optimal solution of (37).

*Proof:* Since  $C\Xi(k|k)$  in (36) is a one-dimensional interval, one can solve problem (37) by adopting the same strategy adopted in Theorem 1 for solving problem (20) in the case of first-order systems. In particular, by using (25), the optimal quantizer parameters in (23)-(24) can be rewritten as

$$\tau_c(k) = \frac{l(k|k-1) + r(k|k-1)}{2}, \quad (41)$$

$$\Delta(k) = \frac{r(k|k-1) - l(k|k-1) - 2\delta_v}{d+1}, \quad (42)$$

where  $l(k|k-1)$  and  $r(k|k-1)$  are, respectively, the infimum and the supremum of the interval  $\Xi(k|k-1)$ , namely the predicted feasible state set in the case of first-order systems. By observing that  $\bar{l}(k)$ ,  $\bar{r}(k)$  in (38) are the infimum and the supremum of the interval  $C\Xi(k|k-1)$ , (39)-(40) immediately follow from (41)-(42).  $\square$  In words, the choice of the quantizer parameters provided by Theorem 3 corresponds to selecting the sensor thresholds in such a way that the feasible output signal set in (36) turns out to have the same radius, irrespectively of the value taken by the output  $y(k)$ , thus leading to the optimal solution of problem (37).

A question that naturally arises is whether the entire feasible state set  $\Xi(k|k)$  is asymptotically bounded when the quantizer is adapted online according to (39)-(40). First, it can be observed that this property trivially holds when system (11) is asymptotically stable. Indeed, even in the least informative scenario in which no measurement set  $\mathcal{M}(k)$  is able to reduce the size of the feasible set, namely  $\mathcal{M}(k) \supseteq \Xi(k|k-1)$ ,  $\forall k \geq 0$ , from (18)-(19) one has

$$\Xi(k+1|k+1) = A\Xi(k|k) \oplus \delta_w G\mathcal{B}_\infty.$$

Then, if  $A$  is asymptotically stable, it turns out that  $\Xi(k|k)$  is asymptotically included in the bounded set  $\sum_{i=0}^{+\infty} A^i \delta_w G\mathcal{B}_\infty$  (see, e.g., [46, 47]).

When the stability assumption is not enforced, the following general result holds.

**Theorem 4** Assume matrix  $A$  is nonsingular and system (11)-(12) is observable. Define the matrix

$$\Omega = \begin{bmatrix} C \\ CA^{-1} \\ \vdots \\ CA^{-n+1} \end{bmatrix} \quad (43)$$

and the vector  $\alpha = CA\Omega^{-1}$ . Let  $\eta^* > 0$  be such that the polynomial

$$q(z) = z^n - \eta \sum_{i=1}^n |\alpha_i| z^{n-i} \quad (44)$$

has all the roots strictly inside the unit circle, for all  $\eta \in [0, \eta^*)$ . Then, if the quantizer parameters are chosen according to (39)-(40), with  $d \in \mathbb{N}$  such that

$$d > \frac{1}{\eta^*} - 1 \quad (45)$$

then the feasible state set  $\Xi(k|k)$  is asymptotically bounded, i.e., there exists  $\rho_\infty > 0$  such that  $\limsup_{k \rightarrow +\infty} \rho(k) \leq \rho_\infty$ . Moreover, for every  $d$  satisfying (45), one has

$$\rho_\infty \leq \max_{w \in \mathcal{B}_\infty} \|\Omega^{-1} D_\infty w\| \quad (46)$$

where

$$D_\infty = \text{diag} \left( \left[ \frac{1}{2} \Delta_\infty + \delta_v \right] \mathbf{1} + \delta_w \beta \right) \quad (47)$$

with

$$\Delta_\infty = \frac{2}{d + 1 - \|\alpha\|_1} \cdot \left\{ \delta_v (\|\alpha\|_1 - 1) + \delta_w \left( \|CG\|_1 + \sum_{h=1}^n |\alpha_h| \beta_h \right) \right\} \quad (48)$$

and  $\beta \in \mathbb{R}^n$  is defined as

$$\beta_1 = 0, \quad \beta_h = \sum_{i=0}^{h-2} \|CA^{-(i+1)}G\|_1, \quad h = 2, \dots, n. \quad (49)$$

*Proof:* See Appendix .2. □

Theorem 4 provides a bound to the number of thresholds for which asymptotic boundedness of the feasible state set  $\Xi(k|k)$  is guaranteed. Such a bound is obtained by computing  $\eta^* = \sup\{\eta : q(z) \text{ is Schur}\}$  and then choosing  $d$  as the minimum integer strictly larger than  $\frac{1}{\eta^*} - 1$ . Notice that  $\eta^* > 0$  always exists, thanks to the continuity of the roots of polynomial  $q(z)$  with respect to its coefficients.

In general, the bound (45) may be conservative. However, there are cases in which it turns out to be quite tight, as in the following numerical examples.

**Example 3** Consider system (11)-(12) with

$$A = \begin{bmatrix} a & 1 \\ 0 & a \end{bmatrix}, \quad C = [1 \ 0], \quad G = I_2$$

with  $a \in \mathbb{R}$ ,  $\delta_w = 0.05$  and  $\delta_v = 0$ . The quantizer parameters are updated according to (39)-(40), for different values of  $d$ . Figure 1 reports, for different values of  $a$ : (i) the minimum  $d \in \mathbb{N}$  for which the feasible set  $\Xi(k|k)$ , resulting from the worst-case realization of the quantized output  $y(k)$ , remains asymptotically bounded; (ii) the minimum  $d \in \mathbb{N}$  satisfying (45). It can be observed that the upper bound given by Theorem 4 is only slightly larger than the minimum number of thresholds for which the feasible state is actually bounded. In this example, the upper bound is tight for  $a \geq 2.3$ .

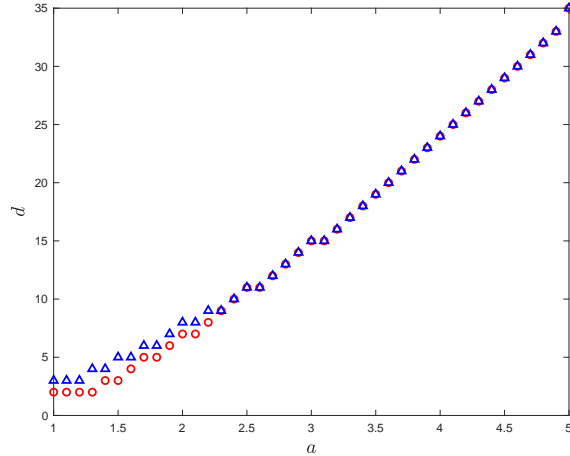


Figure 1: Example 3: minimum  $d$  for which the worst-case  $\Xi(k|k)$  is asymptotically bounded (red circles) and minimum  $d$  satisfying (45) (blue triangles), for different values of  $a$ .

**Remark 3** The lower bound (45) generalizes the condition  $d > a - 1$  in Theorem 2. In fact, for the first-order system (21)-(22),  $q(z)$  in (44) boils down to  $q(z) = z - \eta a$ , for which clearly  $\eta^* = \frac{1}{a}$ , thus leading to  $d > a - 1$  in (45). To the best of the authors' knowledge, in stochastic state estimation of  $n$ -th order systems, a lower bound on the number of thresholds guaranteeing boundedness of the covariance of the state estimation error is still an open problem.

## 6 Threshold selection based on set approximations

The main drawback of the threshold selection mechanism (39)-(40) is that it requires the propagation of the true feasible state set  $\Xi(k|k)$  according to the recursion (18)-(19). Unfortunately, this is not computationally feasible, even for low state dimensions  $n$ . This is a well-known problem in the set membership estimation literature, which led to the development of a number of set approximation techniques. A popular approach is based on the choice of a class of approximating sets  $\Pi$ , from which an outer approximation of the true feasible set is selected at each time  $k$  through the recursion

$$\Pi(k|k) \supseteq \Pi(k|k-1) \bigcap \mathcal{M}(k) \quad (50)$$

$$\Pi(k+1|k) \supseteq A\Pi(k|k) \oplus \delta_w G\mathcal{B}_\infty \quad (51)$$

which is initialized by picking a  $\Pi(0|-1) \supseteq \Xi(0|-1)$ . Many different set classes have been considered in the literature, including ellipsoids [27-29], parallelotopes [30], zonotopes [31-34] and constrained zonotopes [35-37].

When an outer approximation of the feasible set is available, one can design the quantizer thresholds by applying the ideas developed in Section 5 to the approximating set  $\Pi(k|k-1)$ . In particular,  $\tau_c(k)$  and  $\Delta(k)$  can still be chosen according to (39)-(40), where  $\bar{l}(k)$  and  $\bar{r}(k)$  are computed as

$$\bar{l}(k) = \inf_{x \in \Pi(k|k-1)} Cx, \quad \bar{r}(k) = \sup_{x \in \Pi(k|k-1)} Cx. \quad (52)$$

Notice that  $\bar{l}(k)$  and  $\bar{r}(k)$  are easy to compute when the approximating sets  $\Pi$  are parallelotopes or zonotopes. If  $x_c(k|k-1)$  and  $T(k|k-1)$  denote respectively the center and the generator matrix associated to  $\Pi(k|k-1)$ , according to the notation in (5) and (8), one gets

$$\bar{l}(k) = Cx_c(k|k-1) - \|CT(k|k-1)\|_1 \quad (53)$$

$$\bar{r}(k) = Cx_c(k|k-1) + \|CT(k|k-1)\|_1 \quad (54)$$

and hence (39)-(40) boil down to

$$\tau_c(k) = Cx_c(k|k-1), \quad (55)$$

$$\Delta(k) = \frac{2}{d+1}(\|CT(k|k-1)\|_1 - \delta_v), \quad (56)$$

which can be easily computed at each time step. When constrained zonotopes (9) are used as approximating sets, the computation of  $\bar{l}(k)$  and  $\bar{r}(k)$  in (52) requires to solve two linear programs.

## 7 Numerical examples

In this section, the effectiveness of the threshold adaptation based on (55)-(56) is demonstrated on numerical examples.

### 7.1 Case study: double oscillator

We consider the double-spring mechanical system proposed in [39]. The nominal continuous-time model has been discretized with sampling time 0.1 s. The resulting matrices in (11)-(12) are

$$A = \begin{bmatrix} 0.9021 & 0.0967 & 0.0488 & 0.0016 \\ -1.9177 & 0.9021 & 0.9507 & 0.0488 \\ 0.0488 & 0.0016 & 0.9508 & 0.0983 \\ 0.9507 & 0.0488 & -0.9671 & 0.9508 \end{bmatrix},$$

$$G = \begin{bmatrix} 0 & 0 \\ 0.1 & 0 \\ 0 & 0 \\ 0 & 0.1 \end{bmatrix}, \quad C = [ 0 \ 0 \ 1 \ 0 ].$$

The discrete-time disturbances  $w(k)$  and  $v(k)$  are generated as uniformly distributed white processes, satisfying (13) and (14), with  $\delta_w = 0.2$  and  $\delta_v = 0.05$ . The initial state is generated randomly within a box of side 5, i.e.,  $x(0) \in 5\mathcal{B}_\infty$ .

In order to test the threshold selection mechanism based on outer approximation of the feasible state sets, illustrated in Section 6, we consider the following recursive set approximation algorithms.

- *Par*, that uses the recursive parallelotopic approximation proposed in [30], in which the intersection step (50) is performed according to the minimum volume criterion devised in [48].
- *Zon*( $o_z$ ), employing zonotopes with maximum order equal to  $o_z$ . The recursive approximation procedure is the one proposed in [31]. The intersection step in (50) is performed according to the minimum volume criterion illustrated in [49]. If the number of generators exceeds  $o_z n$ , the order reduction procedure proposed in [35] is applied.
- *CZ*( $o_c, n_c$ ), using constrained zonotopes with maximum order  $o_c$  and maximum number of constraints  $n_c$ . The recursive approximation procedure and the order reduction technique are those proposed in [35]. The intersection step in (50) is based on the minimization of the Frobenius norm of the zonotope generator matrix.

All operations involving zonotopes and constrained zonotopes have been performed by using the CORA toolbox for Matlab [50].

A first set of experiments is carried out using the algorithm *Par*, with  $d = 5$  thresholds. Figures 2-3 show the state estimates provided by the center of the parallelotope (dashed) and the uncertainty interval associated to each state variable (solid). The latter has been obtained by computing the minimum box containing the current approximating parallelotope and projecting it on the appropriate dimensions. The evolution of the true state variables is shown in red. In Fig. 2,

the results obtained by adapting the quantizer thresholds according to (55)-(56) are reported. For comparison, Fig. 3 shows the same quantities when the quantizer parameters are kept constant and uniformly distributed in the interval  $[-5, 5]$ , which is approximately the range of the output signal  $z(k)$ . It can be clearly seen that the threshold adaptation mechanism is able to significantly reduce the uncertainty associated to the estimates, even for a relatively small number of thresholds. To better appreciate the difference, the uncertainty intervals estimated with adaptive and fixed thresholds, for a portion of the evolution of state variable  $x_1$ , are shown on Figure 4. The evolution of the quantizer parameters (center and resolution) in the case of adaptive thresholds is shown in Figure 5. It can be observed that the center follows quite closely the behavior of the observed state variable  $x_3$ .

In order to evaluate the role of the threshold number  $d$ , the volumes of the approximating parallelotopes and zonotopes are depicted in Fig. 6 as a function of  $d$ . Results are averaged over 10 runs. As expected, the zonotopic approximation provides smaller volumes with respect to the parallelotopic one. The advantage saturates for zonotopes of order 4, which have 16 generators in  $\mathbb{R}^4$ .

To compare the performance of the different set approximation techniques, we consider the average size of the uncertainty associated to the state estimates. Namely, the radius of the uncertainty interval associated to  $x_i(k)$  is averaged over time  $k$  and over the state variables  $i = 1, \dots, 4$ , for 10 runs involving different initial conditions and disturbance realizations. The time average is performed over the interval  $k \in [50, 200]$  to remove the effect of the initial transient. The results concerning the considered approximation techniques are reported in Tables 1-2, for different values of  $d$ . Table 1 refers to the thresholds adapted according to (55)-(56), while Table 2 concerns the case of fixed thresholds. Table 3 reports the relative times for one iteration of each approximation algorithm, with respect to one iteration of *Par*. The average time for one iteration of *Par* was  $0.16\text{ ms}$  on a computer equipped with Apple M2 CPU and 24 GB of RAM. Clearly, the computational burden of *Zon* and *CZ* algorithms can be triggered by acting on the zonotope order and, for *CZ*, on the number of equality constraints, which in the considered tests has been kept equal to 10.

The benefit of the threshold selection mechanism is apparent, not only in terms of uncertainty size, but also for the number of thresholds. Indeed, uncertainty intervals do not significantly decrease for  $d > 10$  when thresholds are adapted, while they keep decreasing (also for  $d > 20$ ) when thresholds are fixed. This suggests that the number of thresholds required to achieve convergence of the state estimation uncertainty is much higher when thresholds are not adapted.

Concerning the different techniques, constrained zonotopes yield smaller uncertainty intervals, as expected, at the price of a much higher computational burden. Uncertainties provided by the parallelotopic and zonotopic approximations are quite close, with the former approach providing a good trade off between quality of the estimates and required computational effort.

## 7.2 Randomly generated multivariable systems

The adaptive threshold selection procedure has been tested on randomly generated multi-input multi-output linear systems, with  $n = 5$  states. The systems are asymptotically stable and fed with  $m = 3$  input signals  $w(k)$  which are generated as sum of sinusoids with randomly chosen frequencies, corrupted by uniformly distributed white process disturbances satisfying (13) with  $\delta_w = 0.1$ . Quantized measurements of 3 output signals  $z_i(k) = C_i x(k) + v_i(k)$ ,  $i = 1, 2, 3$  are collected, with uniformly distributed white noise  $v_i(k)$  satisfying (14) with  $\delta_v = 0.1$ . For each quantized measurement, adaptive thresholds have been selected according to the procedure proposed in Section 6, based on outer approximation of the feasible state sets. In all recursive set approximation algorithms, quantized measurements are processed sequentially, i.e., step (50) is repeated for each feasible measurement set  $\mathcal{M}_i(k)$  corresponding to the quantized measurement  $y_i(k) = \sigma(z_i(k))$ .

Tables 4-5 report the results of simulations performed on 100 randomly generated systems, each one lasting 100 time instants. The radius of the uncertainty interval associated to state estimates is shown, for different number of thresholds  $d$ . Results are averaged with respect to time, state

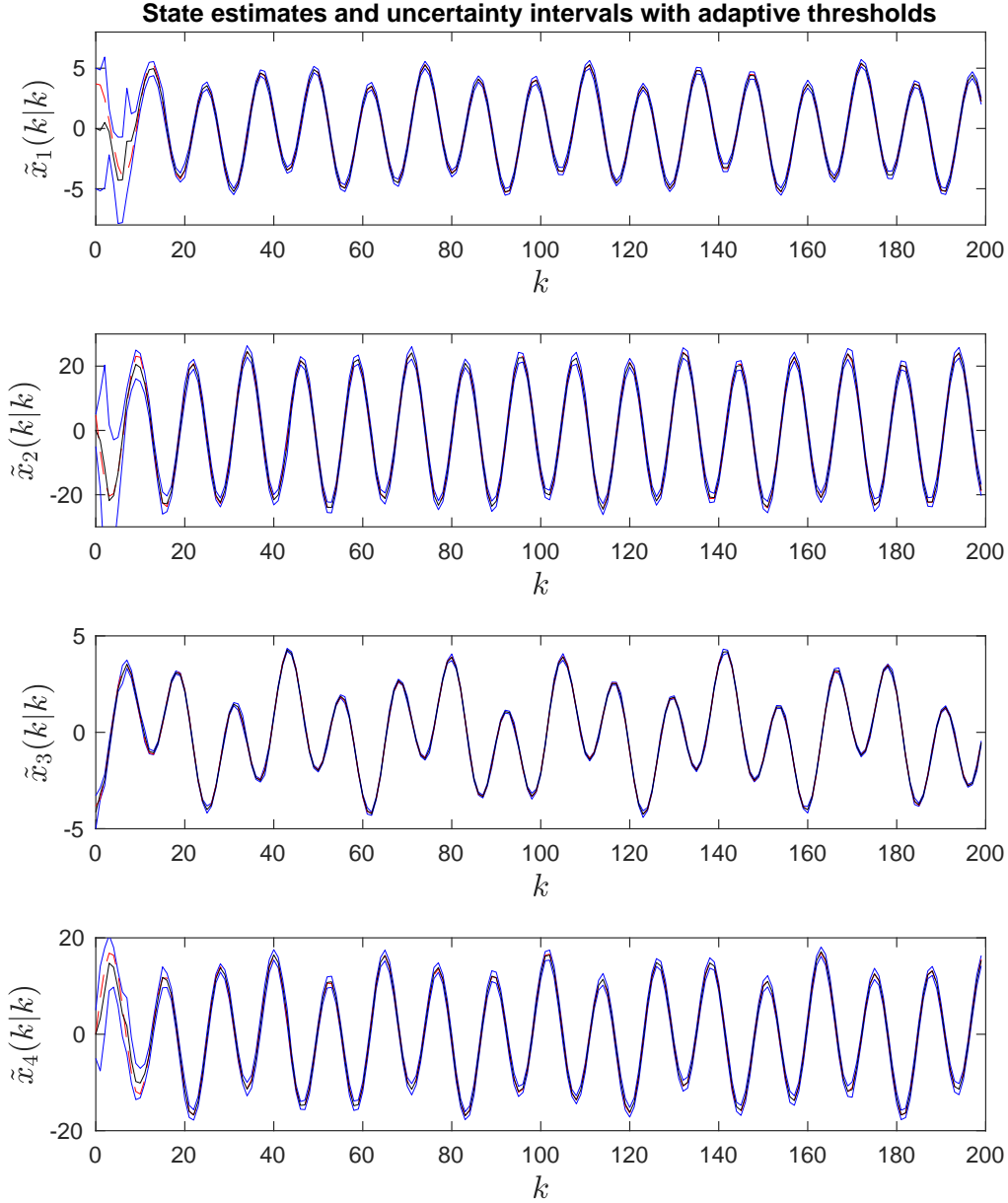


Figure 2: State estimates (black) and uncertainty bounds (blue) for the *Par* algorithm with  $d = 5$  adaptive thresholds. True states are in dashed red.

variables and tested systems. The employed set approximation techniques are the same as in Section 7.1. The order of zonotopes has been limited to 4 because negligible benefits are obtained by increasing such value. For similar reasons  $n_c = 5$  constraints have been used for constrained zonotopes. According to the definition of order for constrained zonotopes, this corresponds to 15 generators for  $CZ(2, 5)$  and 25 generators for  $CZ(4, 5)$ .

Table 4 refers to the case of adaptive thresholds, while those in Table 5 concern a scenario in which thresholds are kept constant. In order to reduce the uncertainty in the latter scenario, for each randomly generated system the thresholds have been chosen equally spaced in the exact range of the unaccessible output signal  $z(k)$ . Nevertheless, it can be seen that adaptive thresholds outperform constant ones. On average, the size of state uncertainty is about three times smaller when thresholds are tuned online with respect to when they are fixed. Notice that this happens

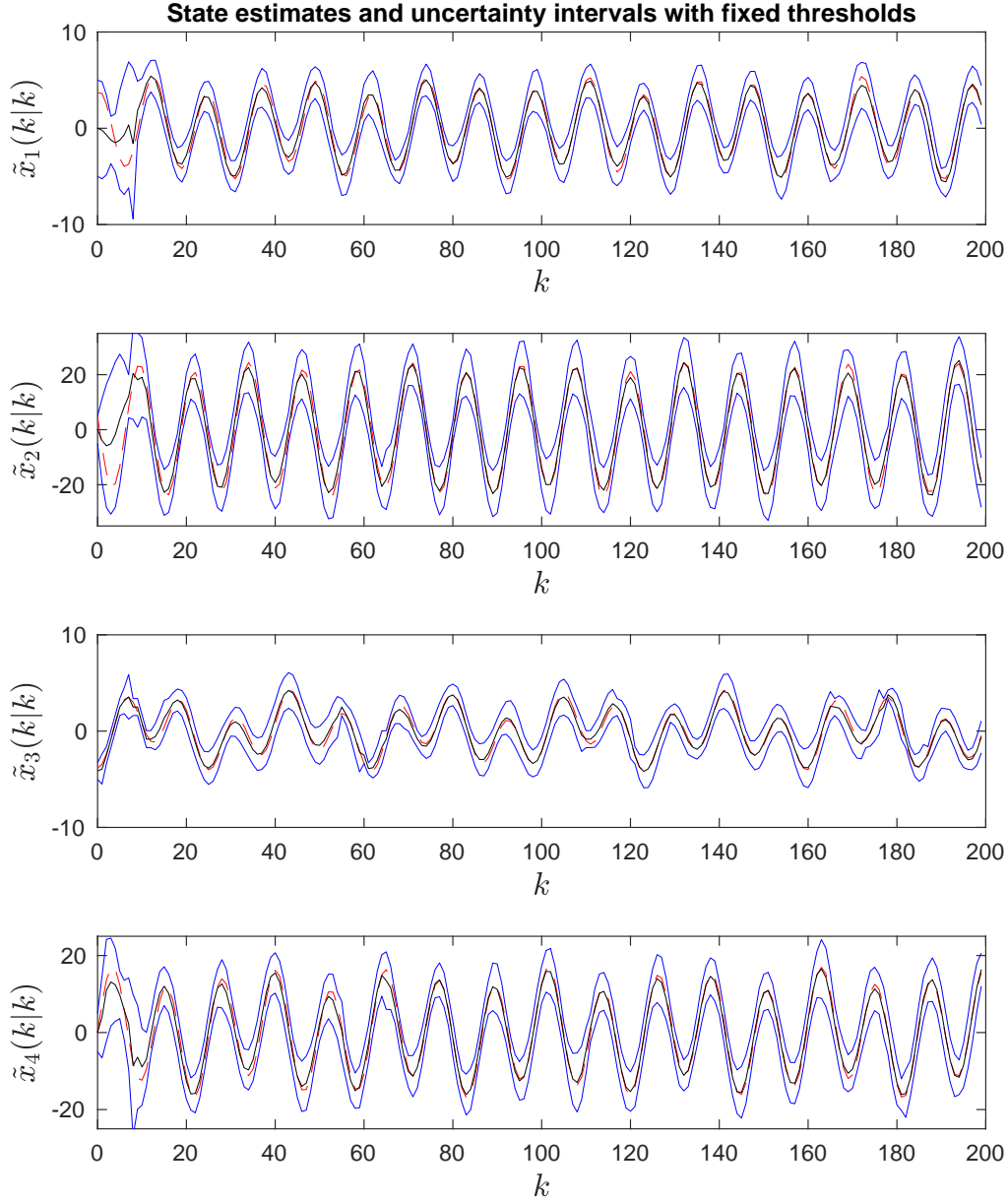


Figure 3: State estimates (black) and uncertainty bounds (blue) for the *Par* algorithm with  $d = 5$  fixed thresholds. True states are in dashed red.

almost irrespectively of both the number of thresholds and the adopted set approximation technique. The average relative times taken by one iteration of each algorithm with respect to that taken by one iteration of *Par* (equal to  $0.2\text{ms}$ ), are reported in Table 6. It is confirmed that constrained zonotopes provide the smallest uncertainty, but they involve a high computational burden. For this study, zonotopes of order 2 seem to be the best compromise between quality of the state estimates and required computational effort.

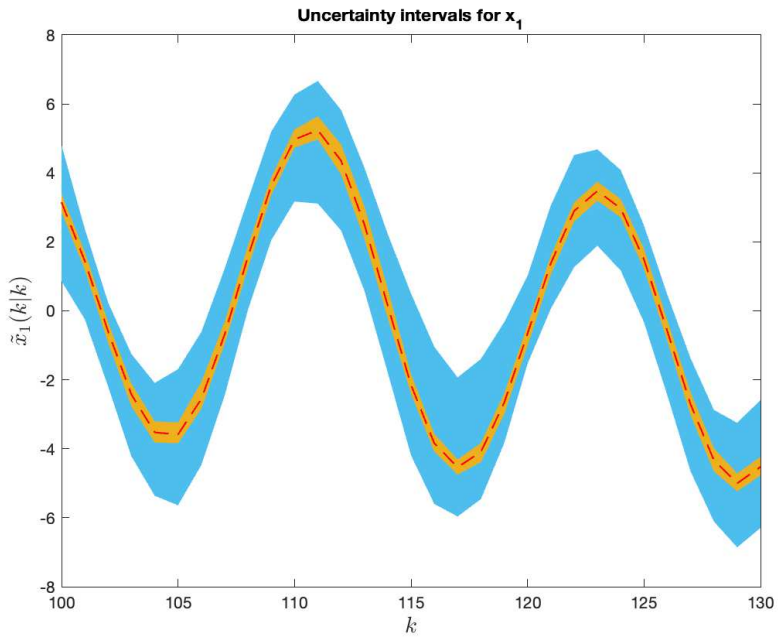


Figure 4: Estimated uncertainty intervals for state  $x_1$ , resulting from fixed (azure) and adaptive (orange) thresholds. The true state value is in red.

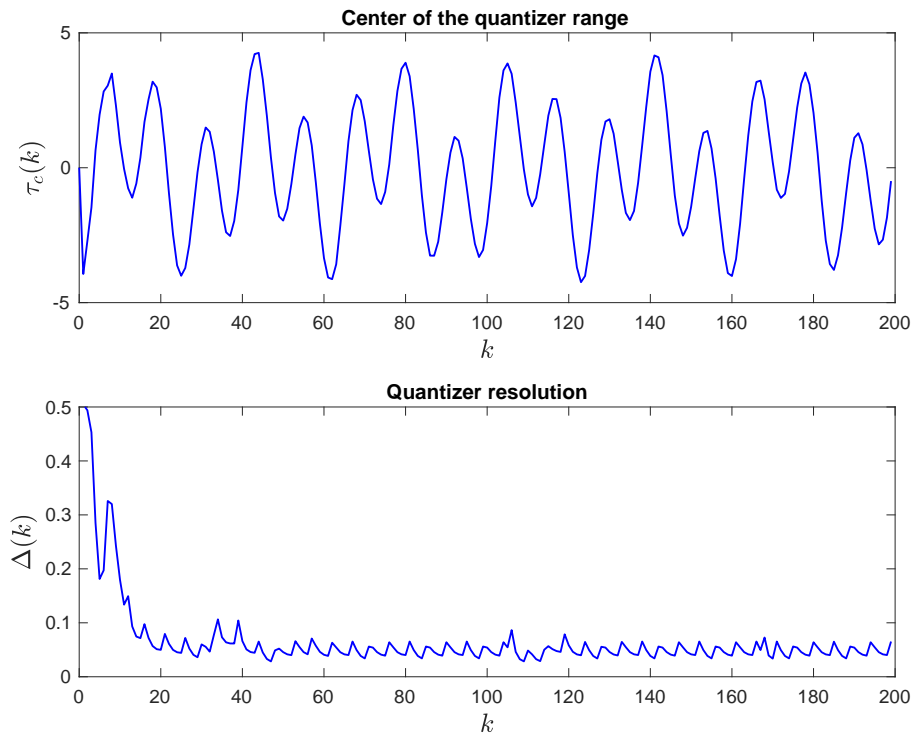


Figure 5: Evolution of the quantizer parameters with  $d = 5$  adaptive thresholds: range center  $\tau_c(k)$  (upper); resolution  $\Delta(k)$  (lower).

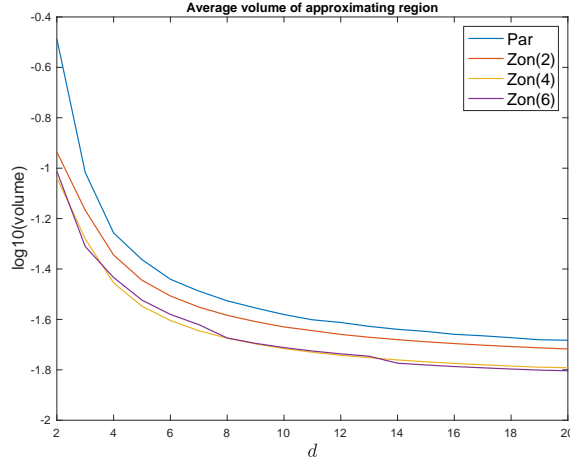


Figure 6: Log-volumes of approximating regions for different number of thresholds  $d$ .

$d$	$Par$	$Zon(2)$	$Zon(4)$	$Zon(6)$	$d$	$CZ(2, 10)$	$CZ(4, 10)$	$CZ(6, 10)$
3	0.93	0.78	0.66	0.62	3	0.56	0.5	0.46
5	0.76	0.66	0.58	0.54	5	0.5	0.43	0.41
10	0.69	0.59	0.52	0.49	10	0.41	0.35	0.32
15	0.67	0.57	0.50	0.48	15	0.38	0.32	0.30
20	0.66	0.56	0.50	0.47	20	0.36	0.31	0.29

Table 1: Average uncertainty associated to the state estimates for  $d$  adaptive thresholds.

$d$	$Par$	$Zon(2)$	$Zon(4)$	$Zon(6)$	$d$	$CZ(2, 10)$	$CZ(4, 10)$	$CZ(6, 10)$
3	5.68	7.55	6.41	6.37	3	2.43	2.28	2.24
5	4.54	4.96	5.01	4.94	5	1.93	1.81	1.75
10	2.87	3.08	3.01	2.93	10	1.46	1.39	1.35
15	2.27	2.35	2.21	2.15	15	1.19	1.11	1.07
20	1.93	1.92	1.84	1.77	20	1.05	0.98	0.96

Table 2: Average uncertainty associated to the state estimates for  $d$  fixed thresholds.

$Par$	$Zon(2)$	$Zon(4)$	$Zon(6)$	$CZ(2, 10)$	$CZ(4, 10)$	$CZ(6, 10)$
1	2.9	17.8	90.5	1879.9	3313.8	4858.5

Table 3: Average relative times for one iteration of each algorithm, with respect to one iteration of  $Par$ .

## 8 Conclusions

A new approach to the selection of adaptive thresholds for state estimation with quantized measurements has been proposed. The method relies on the set membership estimation paradigm: thresholds are chosen in such a way to minimize the size of the feasible state set, and hence the uncertainty affecting the state estimates. It has been shown that a computationally cheap solution can be derived by exploiting set approximations based on parallelotopes or zonotopes. Numerical results show that remarkable uncertainty reductions are achieved with respect of quantizers with fixed thresholds. Future developments of this research may concern more accurate quantization schemes for multi-output systems, taking into account the actual shape of the feasible measure-

$d$	$Par$	$Zon(2)$	$Zon(4)$	$CZ(2, 5)$	$CZ(4, 5)$
3	1.44	0.75	0.77	0.44	0.42
5	0.97	0.54	0.51	0.36	0.34
10	0.62	0.41	0.39	0.29	0.27
15	0.53	0.37	0.35	0.27	0.25
20	0.48	0.35	0.34	0.26	0.24

Table 4: Randomly generated systems: average uncertainty associated to the state estimates for  $d$  adaptive thresholds.

$d$	$Par$	$Zon(2)$	$Zon(4)$	$CZ(2, 5)$	$CZ(4, 5)$
3	5.52	1.98	1.36	1.09	0.87
5	3.08	1.62	1.22	0.97	0.81
10	2.01	1.26	1.03	0.82	0.71
15	1.56	1.07	0.93	0.72	0.65
20	1.35	0.97	0.87	0.67	0.61

Table 5: Randomly generated systems: average uncertainty associated to the state estimates for  $d$  fixed thresholds.

$Par$	$Zon(2)$	$Zon(4)$	$CZ(2, 5)$	$CZ(4, 5)$
1	2.9	4.8	2042.4	3521.8

Table 6: Randomly generated systems: average relative times for one iteration of each approximation algorithm, with respect to one iteration of  $Par$ .

ment set generated by multiple output measurements. Another aspect deserving more insight is the trade off between the state estimation performance and the complexity of the approximating sets. In this respect, simple sets like ellipsoids or interval hulls may be considered. The asymptotic boundedness of the state estimation error provided by recursive set approximation techniques is a further topic that requires deeper investigations.

## .1 Proof of Proposition 1

Let  $y \in \mathcal{S}(p, c)$  and  $w \in \mathbb{R}^m$  such that  $w \in \mathcal{B}_\infty$ . Set  $x = Ay + \gamma Gw$ . Then

$$\begin{aligned} |p'A^{-1}x - c| &= |p'y - c + \gamma p'A^{-1}Gw| \\ &\leq |p'y - c| + \gamma \sup_{w \in \mathcal{B}_\infty} |p'A^{-1}Gw| \leq 1 + \gamma \|p'A^{-1}G\|_1. \end{aligned}$$

Conversely, let  $x$  be such that

$$|p'A^{-1}x - c| \leq 1 + \gamma \|p'A^{-1}G\|_1. \quad (57)$$

Set  $y = A^{-1}(x - \gamma G\bar{w})$ , for some  $\bar{w}$ . We need to show that it is always possible to choose  $\bar{w} \in \mathcal{B}_\infty$  so that  $y \in \mathcal{S}(p, c)$ , and hence  $x = Ay + \gamma G\bar{w} \in \mathcal{AS}(p, c) \oplus \gamma G\mathcal{B}_\infty$ . Consider the case  $p'A^{-1}x - c \geq 0$ . Then choose  $\bar{w}$  such that

$$\bar{w}_i = \text{sign}\{(p'A^{-1}G)_i\} \frac{\max\{p'A^{-1}x - c - 1, 0\}}{\gamma \|p'A^{-1}G\|_1}.$$

for  $i = 1, \dots, m$ , with  $(v)_i$  denoting then  $i$ -th entry of vector  $v$ . From (57),  $\bar{w} \in \mathcal{B}_\infty$ . Moreover,

$$\begin{aligned} p'y - c &= p'A^{-1}x - c - \gamma p'A^{-1}G\bar{w} \\ &= p'A^{-1}x - c - \max\{p'A^{-1}x - c - 1, 0\} \end{aligned}$$

which implies  $0 \leq p'y - c \leq 1$  and hence  $y \in \mathcal{S}(p, c)$ . The case in which  $p'A^{-1}x - c \leq 0$  can be treated analogously.

## .2 Proof of Theorem 4

In order to prove the theorem, we need to introduce some lemmas.

**Lemma 1** *Let (39)-(40) hold. Then, for any value taken by  $y(k)$  one has*

$$\text{rad}\left(C\Xi(k|k-1) \cap C\mathcal{M}(k)\right) = \frac{1}{2}\Delta(k) + \delta_v. \quad (58)$$

Moreover, the interval  $C\Xi(k|k-1) \cap C\mathcal{M}(k)$  does not change if the feasible measurement set (17) is rewritten as

$$\mathcal{M}(k) = \left\{ x \in \mathbb{R}^n : |Cx - q(k)| \leq \frac{1}{2}\Delta(k) + \delta_v \right\} \quad (59)$$

for some  $q(k) \in \mathbb{R}$ .

*Proof:* From (38) one has  $C\Xi(k|k-1) = [\bar{l}(k), \bar{r}(k)]$ . By substituting (16) into (17), with  $\tau_c$  and  $\Delta$  given by (39)-(40), one gets

$$\begin{aligned} \mathcal{M}(k) = \{ x \in \mathbb{R}^n : \\ & Cx \leq \bar{l}(k) + \Delta(k) + 2\delta_v \quad \text{if } y(k) = 0; \\ & \bar{l}(k) + i\Delta(k) < Cx \leq \bar{l}(k) + (i+1)\Delta(k) + 2\delta_v \\ & \quad \text{if } y(k) = i, 1 \leq i \leq d-1; \\ & Cx > \bar{r}(k) - \Delta(k) - 2\delta_v \quad \text{if } y(k) = d \}. \end{aligned} \quad (60)$$

Then, (58) follows by noticing that the interval  $C\Xi(k|k-1) \cap C\mathcal{M}(k)$  has always the same length  $\Delta(k) + 2\delta_v$ , for every possible value taken by  $y(k)$ . It is also easy to check that  $C\Xi(k|k-1) \cap C\mathcal{M}(k)$  does not change if in (60) we add the further constraints  $Cx \geq \bar{l}(k)$  when  $y(k) = 0$  and  $Cx \leq \bar{r}(k)$  for  $y(k) = d$ . Hence,  $\mathcal{M}(k)$  in (60) can be rewritten as in (59).  $\square$

Consider the feasible measurement set  $\mathcal{M}(k-h)$ , for  $h = 1, 2, \dots$ . By using (11) iteratively, one can propagate such a set  $h$  steps ahead, thus obtaining the set of states  $x(k)$  compatible with the measurement  $y(k-h)$ , which we denote by  $\mathcal{M}(k|k-h)$  and is given by

$$\mathcal{M}(k|k-h) = A^h \mathcal{M}(k-h) \oplus \delta_w \sum_{i=0}^{h-1} A^{h-1-i} G B_\infty. \quad (61)$$

**Lemma 2** *Let (39)-(40) hold. Then, the  $h$ -step ahead propagated measurement set in (61) takes on the form*

$$\begin{aligned} \mathcal{M}(k|k-h) = \{ x \in \mathbb{R}^n : & |CA^{-h}x - q(k-h)| \\ & \leq \frac{1}{2}\Delta(k-h) + \delta_v + \delta_w \sum_{i=0}^{h-1} \|CA^{-(i+1)}G\|_1 \}. \end{aligned} \quad (62)$$

*Proof:* From Lemma 1,  $\mathcal{M}(k-h)$  can be written as in (59), i.e. as the strip

$$\mathcal{M}(k-h) = \mathcal{S}\left(\frac{C}{\frac{1}{2}\Delta(k-h) + \delta_v}, \frac{q(k-h)}{\frac{1}{2}\Delta(k-h) + \delta_v}\right).$$

Then, (62) follows by applying property (10) to (61).  $\square$

**Lemma 3** *Let the sequence  $x(k) \in \mathbb{R}$  be such that*

$$x(k) \leq a_1 x(k-1) + a_2 x(k-2) + \dots + a_n x(k-n) + b \quad (63)$$

with  $a_i \geq 0$ ,  $i = 1, \dots, n$  and  $b \geq 0$ . Let the polynomial  $z^n - \sum_{i=1}^n a_i z^{n-i}$  be Schur stable. Then, for any initial values  $x(-h)$ ,  $h = 1, \dots, n$ , one has

$$\limsup_{k \rightarrow +\infty} x(k) \leq \frac{b}{1 - \sum_{i=1}^n a_i}. \quad (64)$$

*Proof:* Define the sequence  $\bar{x}(k)$  such that

$$\bar{x}(k) = a_1 \bar{x}(k-1) + a_2 \bar{x}(k-2) + \dots + a_n \bar{x}(k-n) + b \quad (65)$$

with  $\bar{x}(-h) \geq x(-h)$ , for  $h = 1, \dots, n$ . Let  $\psi(k) = \bar{x}(k) - x(k)$ . From (63) and (65) one has

$$\psi(k) \geq a_1 \psi(k-1) + a_2 \psi(k-2) + \dots + a_n \psi(k-n).$$

Being  $\psi(-h) \geq 0$ , for  $h = 1, \dots, n$ , and  $a_i \geq 0$ ,  $i = 1, \dots, n$ , one has  $\psi(k) \geq 0$ ,  $\forall k \geq 0$  and hence  $x(k) \leq \bar{x}(k)$ ,  $\forall k \geq 0$ . From asymptotic stability of system (65), one gets

$$\lim_{k \rightarrow +\infty} \bar{x}(k) = \frac{b}{1 - \sum_{i=1}^n a_i}$$

from which the result follows.  $\square$

We are now ready to prove Theorem 4. The proof proceeds in three steps: (i) the true feasible set  $\Xi(k|k)$  is bounded by a parallelotope generated by the last  $n$  feasible measurement sets, forward propagated to time  $k$ ; (ii) by exploiting Lemmas 1 and 2 and observability of the system, it is shown that such a parallelotope is bounded at every time  $k$ ; (iii) by using Lemma 3, an asymptotic upper bound on the quantizer adaptive resolution  $\Delta(k)$  is derived, which in turn guarantees asymptotic boundedness of the outer parallelotope, and hence of  $\Xi(k|k)$ .

The first step relies on the observation that at each time  $k$  one has

$$\Xi(k|k) \subseteq \bigcap_{h=0}^{n-1} \mathcal{M}(k|k-h) \quad (66)$$

where  $\mathcal{M}(k|k) = \mathcal{M}(k)$  is given by (59). By noticing that both (59) and (62) are strips, the right hand side in (66) is a parallelotope. Hence,

$$\Xi(k|k) \subseteq \mathcal{P}(k|k) = \mathcal{P}(P(k), c(k)), \quad (67)$$

where the shape matrix  $P(k)$  is given by

$$P(k) = \Lambda(k)^{-1} \Omega \quad (68)$$

in which  $\Lambda(k) = \text{diag}([\lambda(k|k) \ \lambda(k|k-1) \ \dots \ \lambda(k|k-n+1)])$ , with

$$\lambda(k|k-h) = \frac{1}{2} \Delta(k-h) + \delta_v + \delta_w \sum_{i=0}^{h-1} \|CA^{-(i+1)}G\|_1, \quad (69)$$

for  $h = 0, 1, \dots, n-1$ . From (43) one has

$$\Omega = \begin{bmatrix} C \\ CA^{-1} \\ \vdots \\ CA^{-n+1} \end{bmatrix} = \begin{bmatrix} CA^{n-1} \\ CA^{n-2} \\ \vdots \\ C \end{bmatrix} A^{-n+1}.$$

Hence, by nonsingularity of  $A$  and observability of system (11)-(12),  $\Omega$  is nonsingular and therefore the parallelotope  $\mathcal{P}(k|k)$  is bounded for every finite  $k$ . Moreover, by (69), a sufficient condition for

$\mathcal{P}(k|k)$  to be asymptotically bounded is that the sequence  $\Delta(k)$  defined by (40) is asymptotically upper bounded. From (38), by using (19) and (67) one has

$$\bar{l}(k) \geq \inf_{x \in \mathcal{P}(k-1|k-1), w \in \mathcal{B}_\infty} CAx + \delta_w CGw, \quad (70)$$

$$\bar{r}(k) \leq \sup_{x \in \mathcal{P}(k-1|k-1), w \in \mathcal{B}_\infty} CAx + \delta_w CGw. \quad (71)$$

Then, from (40), by applying the property (7), one gets

$$\Delta(k) \leq \frac{2}{d+1} \{ \|CA\Omega^{-1}\Lambda(k-1)\|_1 + \delta_w \|CG\|_1 - \delta_v \}. \quad (72)$$

Now, letting  $\alpha = CA\Omega^{-1}$  and exploiting (69), one gets

$$\begin{aligned} \Delta(k) &\leq \frac{2}{d+1} \left\{ \sum_{h=0}^{n-1} |\alpha_{h+1}| \lambda(k-1|k-1-h) + \delta_w \|CG\|_1 - \delta_v \right\} \\ &= \frac{2}{d+1} \left\{ \sum_{h=0}^{n-1} |\alpha_{h+1}| \left[ \frac{1}{2} \Delta(k-1-h) + \delta_v \right. \right. \\ &\quad \left. \left. + \delta_w \sum_{i=0}^{h-1} \|CA^{-(i+1)}G\|_1 \right] + \delta_w \|CG\|_1 - \delta_v \right\} \\ &= \frac{1}{d+1} \sum_{h=1}^n |\alpha_h| \Delta(k-h) + \bar{\gamma} \end{aligned} \quad (73)$$

with

$$\bar{\gamma} = \frac{2}{d+1} \left\{ \delta_v (\|\alpha\|_1 - 1) + \delta_w \left( \|CG\|_1 + \sum_{h=1}^n |\alpha_h| \beta_h \right) \right\}$$

and  $\beta_h$  given by (49). If  $d$  is chosen so that condition (45) holds, by using Lemma 3 one obtains

$$\limsup_{k \rightarrow +\infty} \Delta(k) \leq \Delta_\infty = \frac{\bar{\gamma}}{1 - \frac{1}{d+1} \|\alpha\|_1}$$

which corresponds to (48). Then, from (68)-(69) one gets  $\limsup_{k \rightarrow +\infty} \Lambda(k) \leq D_\infty$  given by (47).

Finally, (46) follows from (67) by using (6).

## References

- [1] R. E. Curry, *Estimation and Control with Quantized Measurements*. MIT Press, 1970.
- [2] G. N. Nair, F. Fagnani, S. Zampieri, and R. J. Evans, "Feedback control under data rate constraints: An overview," *Proceedings of the IEEE*, vol. 95, no. 1, pp. 108–137, 2007.
- [3] R. W. Brockett and D. Liberzon, "Quantized feedback stabilization of linear systems," *IEEE transactions on Automatic Control*, vol. 45, no. 7, pp. 1279–1289, 2000.
- [4] N. Elia and S. K. Mitter, "Stabilization of linear systems with limited information," *IEEE transactions on Automatic Control*, vol. 46, no. 9, pp. 1384–1400, 2001.
- [5] I. R. Petersen and A. Savkin, "Multi-rate stabilization of multivariable discrete-time linear systems via a limited capacity communication channel," in *Proceedings of the 40th IEEE Conference on Decision and Control*, vol. 1. IEEE, 2001, pp. 304–309.

- [6] S. Azuma and T. Sugie, “Optimal dynamic quantizers for discrete-valued input control,” *Automatica*, vol. 44, no. 2, pp. 396–406, 2008.
- [7] L. Y. Wang, G. G. Yin, J. F. Zhang, and Y. Zhao, *System Identification with Quantized Observations*. Springer, 2010.
- [8] E. Weyer, S. Ko, and M. C. Campi, “Finite sample properties of system identification with quantized output data,” in *Proceedings of the 48th IEEE Conference on Decision and Control, held jointly with the 28th Chinese Control Conference*, December 2009, pp. 1532–1537.
- [9] B. I. Godoy, G. C. Goodwin, J. C. Aguero, D. Marelli, and T. Wigren, “On identification of FIR systems having quantized output data,” *Automatica*, vol. 47, no. 9, pp. 1905–1915, 2011.
- [10] M. Casini, A. Garulli, and A. Vicino, “Input design in worst-case system identification with quantized measurements,” *Automatica*, vol. 48, no. 12, pp. 2997–3007, 2012.
- [11] V. Cerone, D. Piga, and D. Regruto, “Fixed-order FIR approximation of linear systems from quantized input and output data,” *Systems & Control Letters*, vol. 62, no. 12, pp. 1136–1142, 2013.
- [12] G. Bottegal, H. Hjalmarsson, and G. Pillonetto, “A new kernel-based approach to system identification with quantized output data,” *Automatica*, vol. 85, pp. 145–152, 2017.
- [13] W. S. Wong and R. W. Brockett, “Systems with finite communication bandwidth constraints - Part I: State estimation problems,” *IEEE Transactions on Automatic Control*, vol. 42, no. 9, pp. 1294–1299, 1997.
- [14] E. Sviestins and T. Wigren, “Optimal recursive state estimation with quantized measurements,” *IEEE Transactions on Automatic Control*, vol. 45, no. 4, pp. 762–767, 2000.
- [15] M. Fu and C. E. de Souza, “State estimation for linear discrete-time systems using quantized measurements,” *Automatica*, vol. 45, no. 12, pp. 2937–2945, 2009.
- [16] Y. Zhang, Z. Wang, and L. Ma, “Variance-constrained state estimation for networked multi-rate systems with measurement quantization and probabilistic sensor failures,” *International Journal of Robust and Nonlinear Control*, vol. 26, no. 16, pp. 3507–3523, 2016.
- [17] J. C. Aguero, G. C. Goodwin, and J. I. Yuz, “System identification using quantized data,” in *46th IEEE Conference on Decision and Control*, December 2007, pp. 4263–4268.
- [18] L. Y. Wang, G. G. Yin, J. F. Zhang, and Y. Zhao, “Space and time complexities and sensor threshold selection in quantized identification,” *Automatica*, vol. 44, no. 12, pp. 3014–3024, 2008.
- [19] K. Tsumura, “Optimal quantization of signals for system identification,” *IEEE transactions on automatic control*, vol. 54, no. 12, pp. 2909–2915, 2009.
- [20] D. Marelli, K. You, and M. Fu, “Identification of ARMA models using intermittent and quantized output observations,” *Automatica*, vol. 49, no. 2, pp. 360–369, 2013.
- [21] K. You, “Recursive algorithms for parameter estimation with adaptive quantizer,” *Automatica*, vol. 52, pp. 192–201, 2015.
- [22] H. C. Papadopoulos, G. W. Wornell, and A. V. Oppenheim, “Sequential signal encoding from noisy measurements using quantizers with dynamic bias control,” *IEEE Transactions on information theory*, vol. 47, no. 3, pp. 978–1002, 2001.

- [23] J. Fang and H. Li, “Distributed adaptive quantization for wireless sensor networks: From delta modulation to maximum likelihood,” *IEEE Transactions on Signal Processing*, vol. 56, no. 10, pp. 5246–5257, 2008.
- [24] J. M. de la Rosa, R. Schreier, K.-P. Pun, and S. Pavan, “Next-generation delta-sigma converters: Trends and perspectives,” *IEEE Journal on Emerging and Selected Topics in Circuits and Systems*, vol. 5, no. 4, pp. 484–499, 2015.
- [25] F. C. Schweppe, “Recursive state estimation: unknown but bounded errors and system inputs,” *IEEE Transactions on Automatic Control*, vol. 13, pp. 22–28, 1968.
- [26] D. P. Bertsekas and I. B. Rhodes, “Recursive state estimation for a set-membership description of uncertainty,” *IEEE Transactions on Automatic Control*, vol. 16, pp. 117–128, 1971.
- [27] S. Gollamudi, S. Nagaraj, S. Kapoor, and Y. Huang, “Set-membership state estimation with optimal bounding ellipsoids,” in *Proceedings of the international symposium on information theory and its applications*, 1996, pp. 262–265.
- [28] C. Durieu, E. Walter, and B. Polyak, “Multi-input multi-output ellipsoidal state bounding,” *Journal of optimization theory and applications*, vol. 111, no. 2, pp. 273–303, 2001.
- [29] L. El Ghaoui and G. Calafiore, “Robust filtering for discrete-time systems with bounded noise and parametric uncertainty,” *IEEE Transactions on Automatic Control*, vol. 46, no. 7, pp. 1084–1089, 2001.
- [30] L. Chisci, A. Garulli, and G. Zappa, “Recursive state bounding by parallelotopes,” *Automatica*, vol. 32, pp. 1049–1055, 1996.
- [31] T. Alamo, J. M. Bravo, and E. F. Camacho, “Guaranteed state estimation by zonotopes,” *Automatica*, vol. 41, no. 6, pp. 1035–1043, 2005.
- [32] C. Combastel, “Zonotopes and Kalman observers: Gain optimality under distinct uncertainty paradigms and robust convergence,” *Automatica*, vol. 55, pp. 265–273, 2015.
- [33] Y. Wang, Z. Wang, V. Puig, and G. Cembrano, “Zonotopic set-membership state estimation for discrete-time descriptor LPV systems,” *IEEE Transactions on Automatic Control*, vol. 64, no. 5, pp. 2092–2099, 2019.
- [34] M. Althoff and J. J. Rath, “Comparison of guaranteed state estimators for linear time-invariant systems,” *Automatica*, vol. 130, p. 109662, 2021.
- [35] J. K. Scott, D. M. Raimondo, G. R. Marseglia, and R. D. Braatz, “Constrained zonotopes: A new tool for set-based estimation and fault detection,” *Automatica*, vol. 69, pp. 126–136, 2016.
- [36] V. Raghuraman and J. P. Koeln, “Set operations and order reductions for constrained zonotopes,” *Automatica*, vol. 139, p. 110204, 2022.
- [37] B. S. Rego, D. Locatelli, D. M. Raimondo, and G. V. Raffo, “Joint state and parameter estimation based on constrained zonotopes,” *Automatica*, vol. 142, p. 110425, 2022.
- [38] A. A. de Paula, G. V. Raffo, and B. O. Teixeira, “Zonotopic filtering for uncertain nonlinear systems: Fundamentals, implementation aspects, and extensions [applications of control],” *IEEE Control Systems Magazine*, vol. 42, no. 1, pp. 19–51, 2022.
- [39] G. Battistelli, L. Chisci, and S. Gherardini, “Moving horizon estimation for discrete-time linear systems with binary sensors: algorithms and stability results,” *Automatica*, vol. 85, pp. 374–385, 2017.

- [40] Y. Zhang, B. Chen, and L. Yu, “Fusion estimation under binary sensors,” *Automatica*, vol. 115, p. 108861, 2020.
- [41] H. Haimovich, G. C. Goodwin, and J. S. Welsh, “Set-valued observers for constrained state estimation of discrete-time systems with quantized measurements,” in *2004 5th Asian Control Conference (IEEE Cat. No. 04EX904)*, vol. 3. IEEE, 2004, pp. 1937–1945.
- [42] T. Zanma, T. Ohtsuka, and K.-Z. Liu, “Set-based state estimation in quantized state feedback control systems with quantized measurements,” *IEEE Transactions on Control Systems Technology*, vol. 28, no. 2, pp. 550–557, 2018.
- [43] M. Casini, A. Garulli, and A. Vicino, “Set membership state estimation for discrete-time linear systems with binary sensor measurements,” *Automatica*, vol. 159, p. 111396, 2024.
- [44] J. F. Traub, G. W. Wasilkowski, and H. Woźniakowski, *Information-based Complexity*. San Diego: Academic Press, 1988.
- [45] M. Milanese and A. Vicino, “Estimation theory for nonlinear models and set membership uncertainty,” *Automatica*, vol. 27, pp. 403–408, 1991.
- [46] I. Kolmanovsky and E. G. Gilbert, “Theory and computation of disturbance invariant sets for discrete-time linear systems,” *Mathematical problems in engineering*, vol. 4, no. 4, pp. 317–367, 1998.
- [47] F. Blanchini and S. Miani, *Set-theoretic methods in control*. Springer, 2008, vol. 78.
- [48] A. Vicino and G. Zappa, “Sequential approximation of feasible parameter sets for identification with set membership uncertainty,” *IEEE Transactions on Automatic Control*, vol. 41, pp. 774–785, 1996.
- [49] J. M. Bravo, T. Alamo, and E. F. Camacho, “Bounded error identification of systems with time-varying parameters,” *IEEE Transactions on Automatic Control*, vol. 51, no. 7, pp. 1144–1150, 2006.
- [50] M. Althoff, “Guaranteed state estimation in CORA 2021,” in *Proc. of the 8th International Workshop on Applied Verification of Continuous and Hybrid Systems*, 2021.